Hydrogen Bond Indices and Tertiary Structure of Yeast tRNA^{Phe}

M. S. de Giambiagi, M. Giambiagi, and D. M. S. Esquivel

Centro Brasileiro de Pesquisas Físicas Rua Dr. Xavier Sigaud, 150, Urca, 22290 Rio de Janeiro, RJ, Brasil

Z. Naturforsch. **38 c**, 621–630 (1983); received March 29, 1983

tRNA^{Phe}, Tertiary Structure, Hydrogen Bond, Bond Index, Non-Watson-Crick Pairs

The rigidity and stability of the tertiary structure of yeast tRNA^{Phe} is related to a bond index obtained in an IEHT (iterative extended Hückel theory) calculation. The index permits a quantitative estimate of the electron density along the hydrogen bond, having thus an appealing physical meaning. The results indicate that Hoogsteen-type bonds have, as expected, greater electronic population than Watson-Crick type ones. Other non-Watson-Crick pairs, the wobble pair and $G_{15}-C_{48}$, exhibit high values of the index for the NH ... O bond. In the triples, the electron density of the hydrogen bridges does not weaken (compared with the one of the pairs involved). Contour density maps are shown and dipolar moments of pairs and triples are qualitatively discussed.

Introduction

The three-dimensional crystalline structure of yeast phenylanine tRNA has been thoroughly studied in recent years [1, 2]. Much work has also been devoted to tRNA structure by NMR spectroscopy [3, 4] and different theoretical approaches have been proposed to explain this structure [5, 6]. The non-Watson-Crick pair found by Hoogsteen [7] has opened the way to numerous quantum-mechanical studies [8], including theoretical contributions to the interpretation of NMR results [9]. Among the different complex factors responsible for the stability and rigidity of the yeast tRNA^{Phe} tertiary structure, base pairing plays an important part, through hydrogen bonding in pairs and triples [2].

In the present paper, we restrict ourselves to the discussion of the bond indices of some base pairs appearing in yeast tRNA^{Phe}. Such indices [10] represent a quantitative estimate of the electron density along the bridge; they lend themselves to a simple physical interpretation in the Watson-Crick case [11] and predict the allowance for a different pairing of 5-fluorouracil [12].

We shall explore the meaning of a non-Watson-Crick pairing as regards the tertiary structure; for example, whether the electronic population along a non-Watson-Crick hydrogen bond (as Hoogsteen's) differs from that of a Watson-Crick one. To this end, we shall use the IEHT approximation, which has been shown to be satisfactory enough for our purposes [11]. Non-empirical methods are economically prohibitive for such large systems, and both EHT and IEHT are being improved at present with a view to extend their applicability [13].

The present study includes the calculation of more than fifteen pairs of bases (some of which are not reported here) and two triples, considered as supermolecules [14, 15]*.

The consideration of different geometries for some pairs have led us to the conclusion that bond indices are fairly insensitive to geometry, so that we may safely disregard geometry optimization. We shall see that bond indices depend on topology more than on geometry.

The variety of hydrogen bonds appearing in the nonhelical regions of yeast tRNA^{Phe} has drawn the attention of workers in this field. The fact that experimental data published hitherto are far from conclusive [16, 17] makes worthwhile further theoretical contributions to the understanding of its molecular features.

Hydrogen Bond Indices

A bond index formulation [10] has been found appropriate for the IEHT analysis of Watson-Crick hydrogen bonded nucleic acids [11]. The bond index $I_{\mu\nu}$ between atoms μ and ν is defined as [10]

$$I_{\mu\nu} = \sum_{i,j} \sum_{k_\mu, r_\nu} n_i \, x_{ik_\mu} \, y_{ir_\nu} \, n_j \, x_{jr_\nu} \, y_{jk_\mu} \qquad (1)$$

* The calculation involves matrices of order ranging from 81 (A–U or A*–U*) up to 135 (G–G–C) and around 18 CPU h from a 378/158 IBM computer; see [11].

Reprint requests to Prof. Dr. M. Giambiagi.

0341-0382/83/0700-0621 $ 01.30/0

where x_{ik_μ} is the LCAO coefficient of the k_μ-th atomic orbital belonging to the i-th MO and

$$y_{ir_\nu} = \sum_{p_\sigma} S_{p_\sigma r_\nu} x_{ip_\sigma} \tag{2}$$

where S is the overlap matrix. $I_{\mu\nu}$, which is rotationally invariant, may be interpreted as the active charge [10, 18] distributed along both effective and formal bonds between atom μ and all other atoms.

Table I. Bond indices in XH ... Y bonds, (i) pairs, (ii) triples.

	Pair	Fig.	X	Y	I_{XY}	I_{XH}	I_{HY}
(i)							
	A–U	(3a)	N	O	0.026	0.941	0.033
			N	N	0.054	0.897	0.076
	G–C	(3b)	N	O	0.039	0.923	0.051
					0.032	0.932	0.042
			N	N	0.053	0.889	0.077
	A–U	(4a)	N	O	0.038	0.932	0.048
			N	N	0.073	0.868	0.107
	A_{14}–U_8	(4b)	N	O	0.037	0.933	0.047
			N	N	0.073	0.868	0.107
	G_{15}–C_{48}	(5a)	N	O	0.058	0.890	0.081
			N	N	0.052	0.900	0.073
	A–C	(5b)	N	N	0.053	0.901	0.074
					0.054	0.901	0.075
	G_4–U_{69}	(6a)	N	O	0.052	0.901	0.072
					0.054	0.889	0.077
	G–U*	(6b)	O	O	0.065	0.854	0.091
			N	N	0.055	0.885	0.079
			N	O	0.044	0.915	0.059
	G_{46}–G_{22}	(7a)	N	N	0.076	0.859	0.114
			N	O	0.036	0.929	0.046
	A–A	(7b)	N	N	0.056	0.901	0.077
					0.049	0.910	0.068
	C_1–C_2	(8a)	N	N	0.051	0.901	0.074
			N	O	0.056	0.899	0.075
	A*–U*	(8b)	O	N	0.058	0.877	0.081
			N	N	0.054	0.893	0.078
(ii)							
Triple							
A_9–A_{23}–U_{12}	A_9–A_{23}	(9a)	N	N	0.047	0.911	0.066
					0.043	0.911	0.068
	A_{23}–U_{12}		N	O	0.026	0.940	0.033
			N	N	0.054	0.896	0.076
G_{46}–G_{22}–C_{13}	G_{46}–G_{22}	(9b)	N	O	0.036	0.929	0.045
			N	N	0.076	0.859	0.114
	G_{22}–C_{13}		N	O	0.032	0.918	0.044
					0.048	0.889	0.067
			N	N	0.052	0.885	0.073

Table I shows the $I_{\mu\nu}$ values for the atoms involved in the XH ... Y bonds appearing in the different base pairs and triples. Let us recall that in the calculation of the associations in the supermolecular approach the only meaningful intermolecular $I_{\mu\nu}$ values are those which correspond to the hydrogen bonds [11]; this fact, which our present results ratify, strongly reinforces the physical meaning of this quantity. Again, as has been suggested in an early study [19] and obtained in [11], they are of σ nature.

The table gives the pairings appearing in some tRNAs (in particular yeast tRNA^{Phe}). The C_1–C_2 dimer has been included for the sake of comparison with an experimental contour density map (see next section). The labelling (Fig. 1) corresponds to the known sequence given for example by Robertus *et al.* [2], who studied the X-ray structure of yeast tRNA^{Phe} through the isomorphous replacement method with a resolution of 3 Å.

The familiar picture which we reproduce in Fig. 2, is most fitting to our discussion. The base complexes conferring stability and rigidity to the tertiary structure are dominantly of non-Watson-Crick type. As we mentioned in the introduction, we want to see whether this intriguing fact evidences itself in some way through the information which

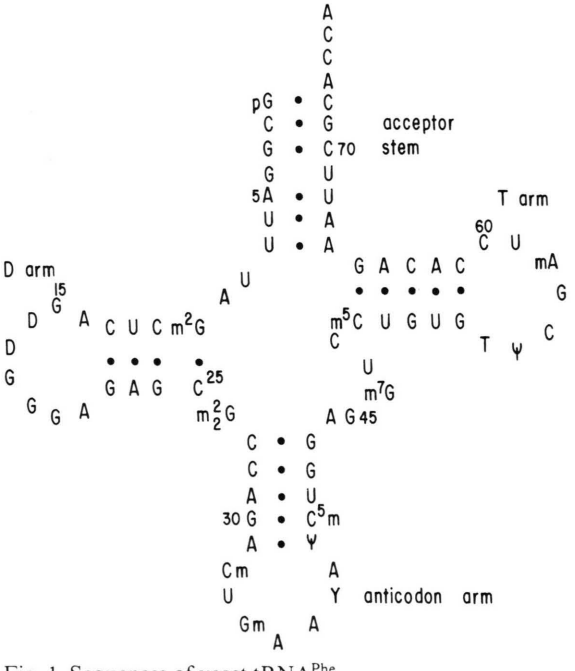

Fig. 1. Sequences of yeast tRNA^{Phe}.

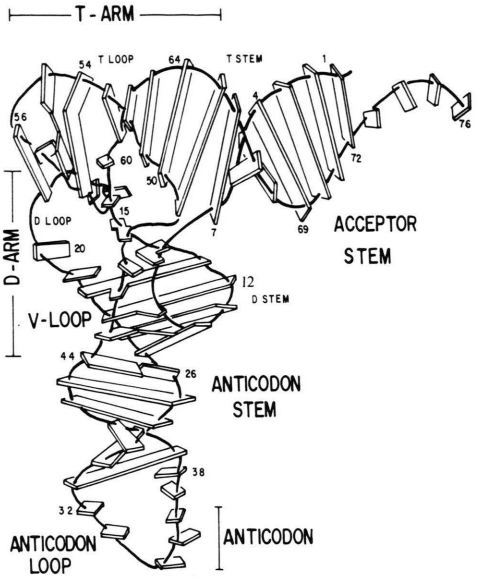

Fig. 2. Orientation of bases in tRNA molecule. Taken from S. H. Kim, in Transfer RNA, S. Altman, ed. (MIT press, Cambridge, Massachusetts, 1978), p. 248.

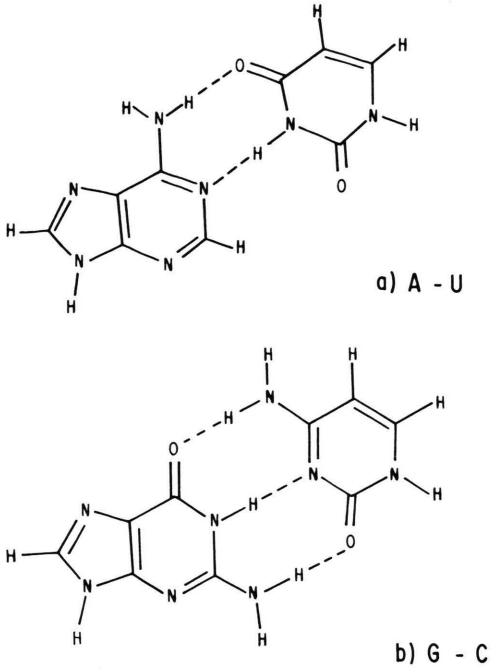

Fig. 3. Watson-Crick pairings.

the I_{XY}'s supply; that is, whether the electronic densities along H bonds in non-Watson-Crick pairings are different or not from the Watson-Crick ones.

Let us remind that in the Watson-Crick pairing (Fig. 3), I_{NN} is *constant* (0.054) [11], while I_{NO} (in NH ... O) increases noticeably from A–T and A–U (~ 0.026) to G–C (0.039). It has already been remarked that there is a need to discriminate the H-donor abilities of the different XY groups, since the points relative to OH, NH and CH fall within well separated regions of the $\Delta\nu_{XH}$ diagrams [20]. The constancy of the NH ... N bond, compared with the NH ... O one seems to be unexpected, however.

Now, the Hoogsteen pairs (Fig. 4) exhibit an appreciably higher I_{NN} value for the direct (*cis*) and reversed (*trans*) conformations; this is in agreement with calculated stabilities [8]. The invariant A_{14}–U_8 pair is of the reversed kind, which apparently is preferred in nature to the direct one. Sundaralingam [21] argues that the construction of the *cis* conformation "would necessitate flipping the adenine base from the preferred anti to the less favoured syn conformation". As our preliminary calculations led to the same I_{XY} values for Watson-Crick A–T and A–U, we have not calculated the *trans* Hoogsteen pair T_{54}–A_{58}.

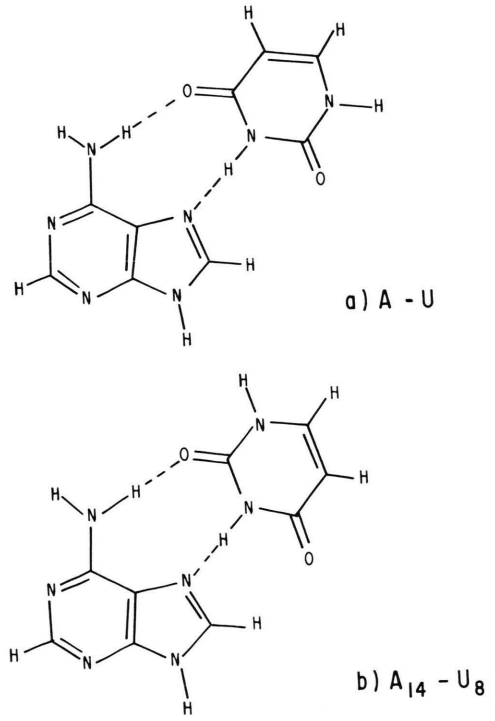

Fig. 4. Direct and reverse Hoogsteen pairings.

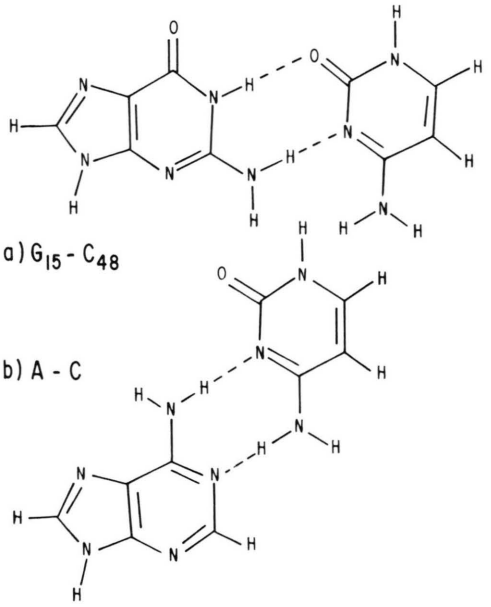

Fig. 5

The pair G_{15}–C_{48} (Fig. 5), which is also invariant, plays an important part in the tertiary structure, for it links loop D with the variable loop, being an apparently unfavourable pairing with only two hydrogen bonds. However, comparing it with the three-bonded G–C pair, I_{NO} is greater by 66%, I_{NN} remaining equal. The G_{15}–C_{48} resonance at the high-field end of the NMR spectrum could correspond to a bonding less deshielding than the normal Watson-Crick one [22]. An exception to the constancy of the G_{15}–C_{48} pair is the A–C pair found for glycine tRNA [2]; for A–C, the two I_{NN} values are quite close to the I_{NN} and I_{NO} values of the G_{15}–C_{48} pair.

The Crick wobble pair (Fig. 6) [23] appearing in the acceptor stem is the only non-Watson-Crick pair in the double helical stems [24]. The I_{XY} results present no objection to the wobble. Let us compare with the G–U* pair, which is the pairing predicted usually for U under enol form [25]. On the one hand, G–U* has three H-bonds with one O–O bond (the only one appearing in the present study) with a relatively high I_{OO} value. On the other hand, both I_{NO}'s of G_4–U_{69} are larger than the corresponding one in G–U*. The NO bonds involving pyrrole-type nitrogens tend to have higher I_{XY} values than those with amino-type nitrogens.

In order to roughly explore the influence of neighbourhood upon the bond index, we have calculated a pair similar to the wobble one, placing artificially an oxygen in uracil's position 6 instead of 4 (a 180° rotation about the axis through C_2 and C_5). Surprisingly, we obtain a decrease, not only for the upper bridge (from $I_{NO} = 0.052$ to 0.041) but also for the lower one (from $I_{NO} = 0.054$ to 0.033). The bond index value is thus related with the pairing positions in a much more intricate fashion than we perceived.

The pair G_{46}–G_{22} (Fig. 7), entering one of the triples, has the same high I_{XY} values as the A–U Hoogsteen pair. Let us name Hoogsteen type pairing the seven-side one and Watson-Crick type pairing, in an extended sense, the six-sided one. Each type of pairing exhibits a constant I_{NN} value except for A–A. The A–A we have reported, which is *not* A_9–A_{23}, is found in some initiator tRNAs and seems to be the one observed in the crystal structure of 9-MeAde [8]. Despite being seven-sided, its I_{NN}'s look as extreme as the six-sided typical values. In turn, the A_9–A_{23} eight sided pair belonging to the triple (Fig. 9) shows the lowest values. It seems thus that seven-sided pairs maximize I_{NN}.

The dimer C_1–C_2 (Fig. 8), which appears in crystalline cytosine monohydrate [26], displays an unusually high I_{NO}, surpassed only by G_{15}–C_{48}

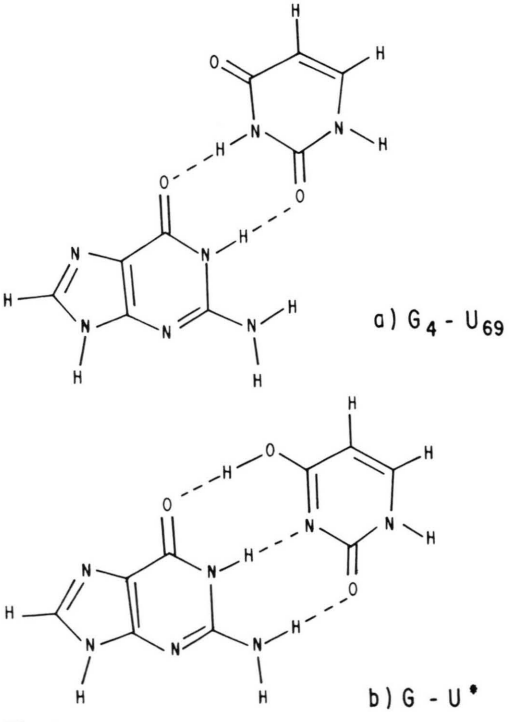

Fig. 6

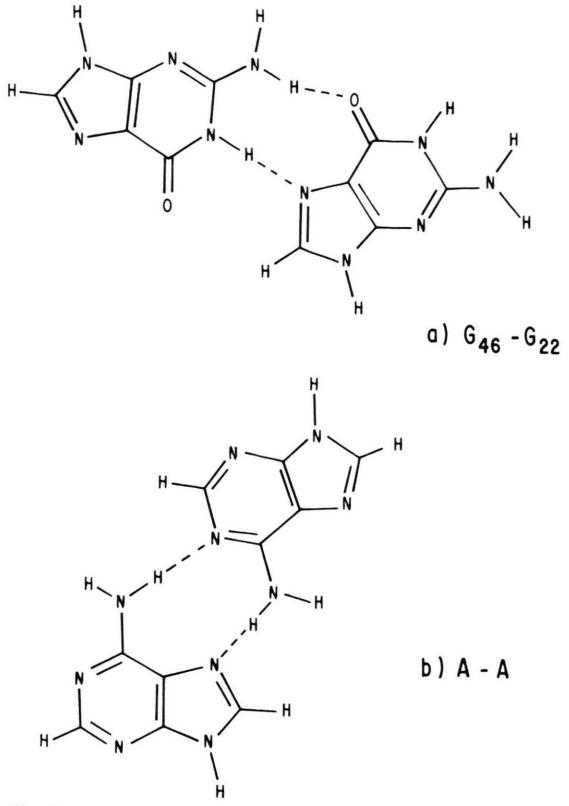

Fig. 7

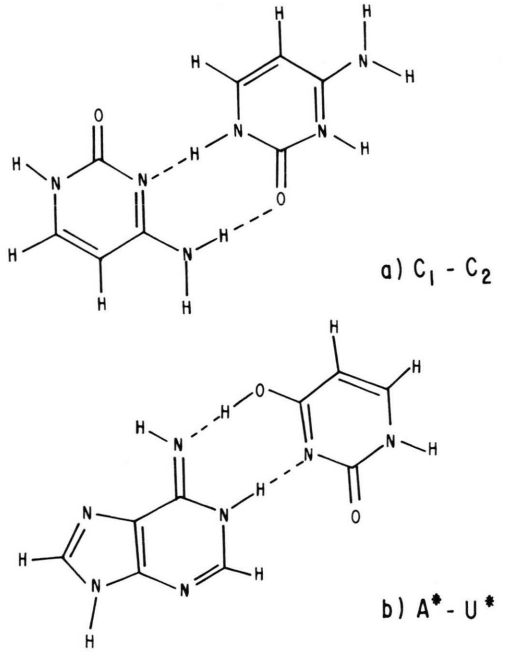

Fig. 8

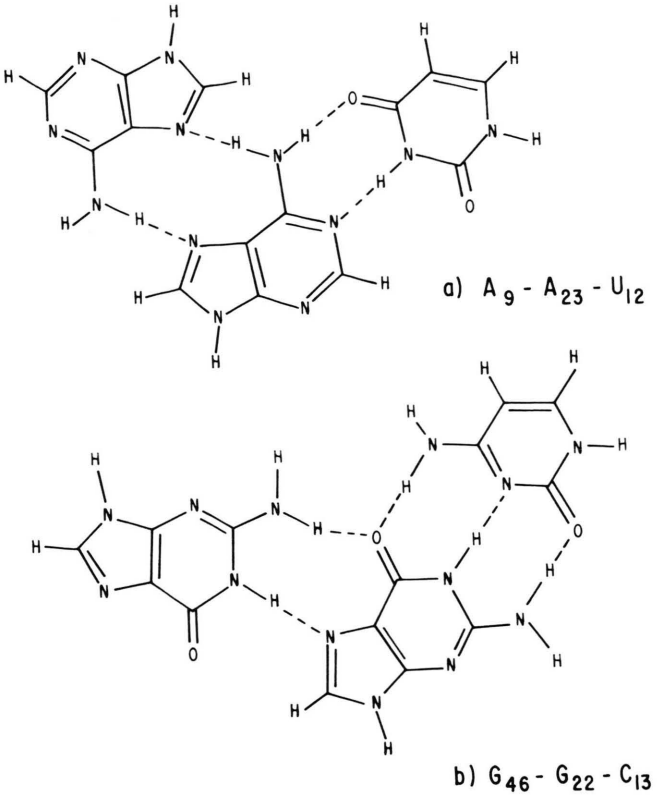

Fig. 9

(see next section), which in turn is equal to I_{ON} in A*–U*; this last pair possesses the only OH ... N bond reported here. Experimental results for dimer formation enthalpies indicate stronger hydrogen bonds for C–C than A–U or A–T [27]; this could be related to the high I_{NO} value which we obtained.

The only classical Watson-Crick pair contributing to the tertiary structure of yeast $tRNA^{Phe}$ is G_{19}–C_{56}. Should a classical Watson-Crick pair appear in this structure, we would expect it to be G–C instead of A–T or A–U for, besides owning three hydrogen bonds, it has higher I_{NO} values. Yet, it has recently been suggested that conformational changes of yeast $tRNA^{Phe}$ induced by various intercalators may entail a weakening of the D-loop-T-loop interaction [28]. Such a weakening would involve the G_{19}–C_{56} pair, which may appear slightly distorted, hence exhibiting a peculiar lability. We shall see immediately that when the Watson-Crick G–C pair enters the G–G–C triple its indices change, while the Watson-Crick A–U pair maintains its values in A–A–U.

When analyzing the behaviour of triples (Fig. 9, Table I (i)), compared to the pairs they include, we conclude that their formation does not involve any loss or dissipation in the hydrogen bond electron density. The A–A pair appearing in A–A–U is eight-sided instead of the seven-sided one reported in Table I (i); its values are lower by about 15%. Nevertheless, I_{NO} in the second NH ... O bond of G–C belonging to the triple, is 50% higher than that of the pair. It is not obvious that the electron density does not weaken under triple formation; this may be a factor for triple stability, which in turn could be related to the significative contribution of the triples to the three-dimensional tRNA structure. Unlike what is expected [19] both hydrogen bonds involving the same oxygen atom in the triple have values close to each other.

We had noticed [11] that the fraction of an electron lost by the NH bond of the separate bases when forming a Watson-Crick pair goes almost entirely to the bridge. This, in line with our present results, appears as a characteristic of the NH bond, not being verified for OH.

It has long been recognized that hydrogen bond formation lengthens the XH distance; the relation between the infrared band due to the XH stretching vibration and the inverse dependence of the XY distance as a function of the bond strength [19] is also well known. In the separate bases, our I_{NH} stays within the range 0.968–0.980 [11] and I_{OH} in U* is 0.936; we see from Table I that in pairs I_{XH} spans from 0.854 (OH in G–U*) up to 0.940 (NH in Watson-Crick A–T and A–U). Actually, the mean I_{XH} value of Table I is 0.90, clearly lower than that of the separate bases. This trend is in satisfactory agreement with experimental results.

The values of Table I suggests a proportionality between I_{XY} and I_{HY}. We have found

$$I_{HN} = (1.44 \pm 0.01)\, I_{NN}; \quad I_{HO} = (1.31 \pm 0.01)\, I_{NO}.$$

There is only one I_{ON} and one I_{OO}. For these, $I_{HN} = 1.40\, I_{ON}$ and $I_{HO} = 1.40\, I_{OO}$ respectively.

Electron-Density Diagrams

Density diagrams are heavily time-consuming. Thus we selected a few significant diagrams and left aside electron density difference maps [29]. We display in Fig. 10 the reversed Hoogsteen A–U pair. The addition of the Watson-Crick G–C diagram is unnecessary to the understanding of Table II, which reports the conjugation curves ϱ together with the I_{XY} values. The conjugation curves for the reversed Hoogsteen A–U pair are higher than those of the Watson-Crick A–U pair, in agreement with the I_{XY} values.

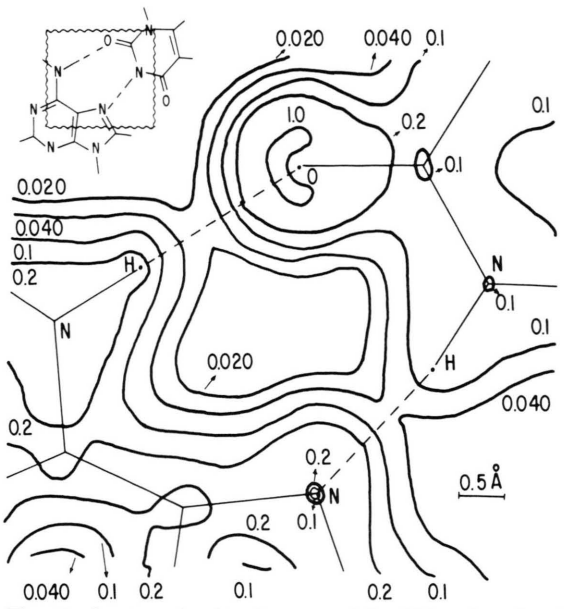

Fig. 10. Contour density diagram of the H-bond region in reversed Hoogsteen A–U, in the molecular plane. Units are e au^{-3}.

Refinement analysis of X-ray diffraction data at 2.5 Å resolution leads to electron density maps of the associations appearing in yeast $tRNA^{Phe}$; previous results were obtained with lower resolution and, as refinement proceeded, the hydrogen bonding regions became clearer [24]. With 2.5 Å resolution, however, the electron density maps show clusters of atoms rather than atoms, so that the conjugation

Table II. Conjugation curves (ϱ) and I_{XY} values.

Base pair	X	Y	ϱ (e au^{-3})	I_{XY}
Watson-Crick A–U [14]	N	O	0.015	0.026
	N	N	0.025	0.054
Hoogsteen A_{14}–U_8	N	O	0.020	0.037
	N	N	0.040	0.073
Watson-Crick G–C	N	O	0.015	0.039
	N	N	0.025	0.053
	N	O	0.015	0.032
C–C dimer	N	N	0.025	0.051
	N	O	0.035	0.056

curves seldom stand out. It is hence difficult to compare our Fig. 10 with the experimental $A_{14}-U_8$ map; furthermore, this map includes the sugar phosphate backbone, which our calculation cannot take into account. However, the conjugation curve corresponding to our enhanced I_{NO} value of $G_{15}-C_{48}$ *is distinctly visible.* In the experimental diagrams for pairs and triples, the contours for any single base look different depending upon the association in which they are involved. Nevertheless, as they are undoubtedly affected by the sugar-phosphate backbone, we cannot separate the effect of the backbone from that of association.

In order to see how association influences the density diagrams, we have drawn cytosine and its dimer (Fig. 11, Table II). The dimerization adopted obeys the model proposed for interpreting structural experimental data of cytosine monohydrate, based on a three-dimensional photographic analysis; an electron density distribution map of cytosine in the molecular plane is obtained from the experimental results [26]. Fig. 11b shows that under association the 0.030 outer contour merely splits into the 0.025 and the 0.035 conjugation curves in the hydrogen bonding region. Although our diagram does not reproduce the detailed experimental structure, its rather delocalized aspect is better visualized in Fig. 11a than in an *ab-initio* diagram of cytosine [30].

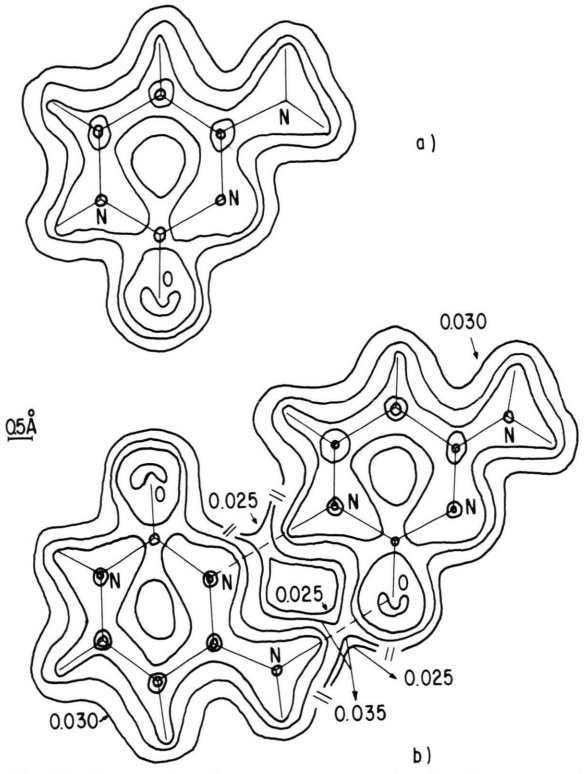

Fig. 11. Comparison between contour density diagrams of cytosine (a) and its dimer (b), in the molecular plane. The contours are respectively, from outside, 0.30, 0.1, 0.2 and 1.0 $e\,au^{-3}$. The 0.030 contour splits into 0.025 and 0.035 in the H-bond region.

Table II suggests a rough proportionality between ϱ and I_{XY}; anyhow, we have found that in an unusual G-5FU pairing the NH ... F bond has a lower I_{XY} and a slightly higher conjugation curve than the OH ... O one [12].

Table III shows the origin of HOMO and LUMO in the pairs and triples of the present calculation. In Ref. [11] we have drawn the HOMO's of the Watson-Crick A–U pair, and those of U and A separately. It is clearly depicted there that HOMO is almost wholly U and arises primarily from uracil's O_4. From the table we see that this behaviour is quite general; association merely changes the orientation of the HOMO's lone pair.

One could have expected the HOMO's to be hybrid lone-pair orbitals, but they are decidedly p orbitals. Recently, through an *ab-initio* calculation, Fukui *et al.* [31] have found a similar feature for the delocalization interaction orbitals of ammonia and methylamine, and suggested that the p nature must be enhanced in order to create a new bond. This is consistent with our results for uracil. HOMO is $2p_\sigma$ for O_4, the position where it tends to enolize. Only when the O_4 position is already enolized, does the HOMO become a $2p$ belonging to O_2, which in turn is thus ready to receive a proton. This behaviour is independent from pairing, for the

Table III. HOMO and LUMO of pairs and triples.

	Fig.	HOMO (σ)	LUMO (π)
A–U	(3a)	U (O_4)	A
G–C	(3b)	C (O)	C
A–U	(4a)	U (O_4)	A
$A_{14}-U_8$	(4b)	U (O_4)	A
$G_{15}-C_{48}$	(5a)	G (O)	C
A–C	(5b)	C (O)	C
G_4-U_{69}	(6a)	G (O)	U
G–U*	(6b)	U (O_2)	U
$G_{46}-G_{22}$	(7a)	G_{46} (O)	G_{22}
A–A	(7b)	A + A	A + A
C_1-C_2	(8a)	C_2 (O)	C_1
A*–U*	(8b)	U (O_2)	U
$A_9-A_{23}-U_{12}$	(9a)	U (O_4)	$A_9 + A_{23}$
$G_{46}-G_{22}-C_{13}$	(9b)	G_{46} (O)	C_{13}

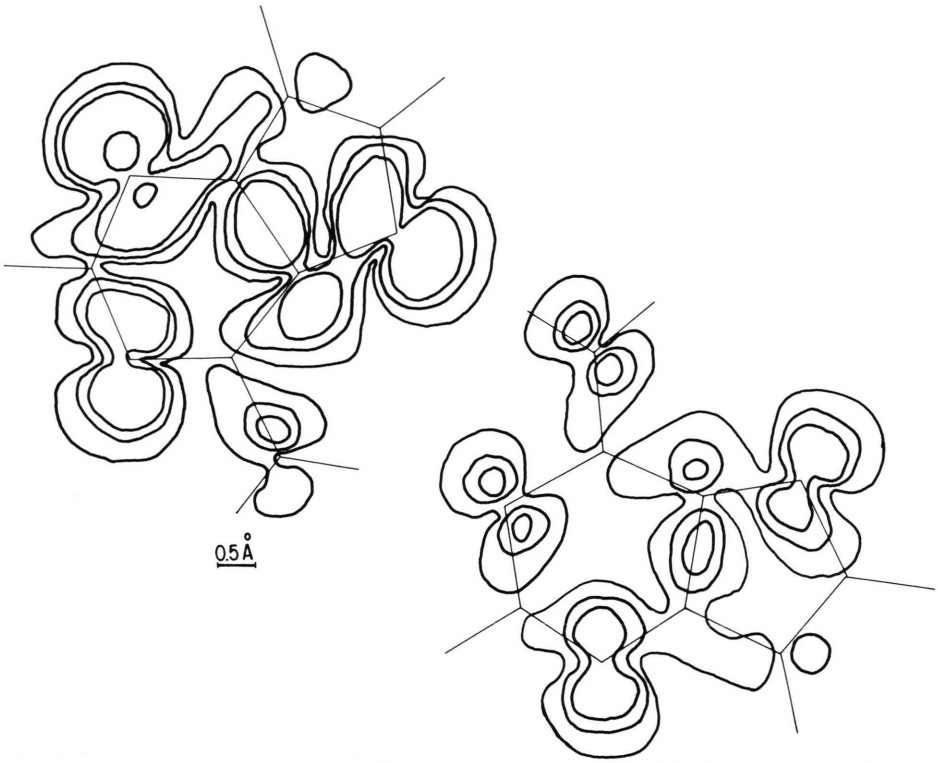

Fig. 12. HOMO of the A–A pair, in the molecular plane. Contours are respectively, from outside, 0.001, 0.005 and 0.01 e au^{-3}.

hydrogen bond is usually too weak an interaction to influence the HOMO's nature, at least within the limits of an IEHT calculation.

Thus, wherever an oxygen is present, HOMO is always a $2p_\sigma$ oxygen orbital, with a coefficient higher than 0.8. This holds both for pairs and triples. LUMO's are all π, and hence delocalized.

Although more frequently HOMO and LUMO originate from different single bases, as has been obtained in a π semiempirical selfconsistent calculation of the G–C pair [32], this is not always the case; in particular our result does not apply for the Watson-Crick G–C base pair. This does not depend on the hydrogen bond. Sometimes the HOMO's oxygen is involved in it, sometimes not.

The A–A dimer, the only pair considered which does not contain oxygen, exhibits an unusual HOMO; it is also σ, but a delocalized one (Fig. 12). Both adenines have diagrams similar to that of the separate base [11]. It is seen that the left base contributes somewhat more than the right one; N_1 enters in the 0.0001 delocalization curve in the first and does not in the second.

Each of the two triples behave differently. In $A_9-A_{23}-U_{12}$, HOMO belongs to uracil, and LUMO is built from both adenines. In $G_{46}-G_{22}-C_{13}$, G_{22} does not take part either in HOMO or in LUMO.

In the separate bases also our HOMO is σ and LUMO is π. Some other calculations differ regarding this prediction [33]. Recently, theoretical studies and analysis of experimental data have indicated the presence of $n-\pi^*$ transitions in the first absorption bands of the bases [34].

Hybridization and Dipole Moments

Table IV reproduces the range of hybridization ratios sp^α. In the bases, the parameter α is <2 for the pyrrole of amino-type N, and >2 for pyridine-type N. Under enolization, uracil's oxygen decreases appreciably its p-character at that position. It has been found [19] that the experimental trend of the energy is reproduced only if the s-character of the orbital associated to atom Y increases as the bond becomes stronger. The range of variation of the results reported in Table IV is too small to relate them to such a strength.

Table IV. Hybridization ratios sp^{α} · α values.

Separate bases		
Pyrrole- or amino-type N		1.85–1.89
Pyridine-type N		2.13–2.23
Carbonyl-O		2.22–2.24
Enol-O		2.06
Pairs and triples (in XH ... Y)		
	X	Y
N	1.90–1.97	2.11–2.21
O	2.07–2.09	2.20–2.23

Oxygen keeps the same α value under association, be it in a X or in a Y role. For the pyridine-type nitrogens (Y atoms) the same occurs, but when they are pyrrole – or amino-type (X atoms) their α value is increased by forming hydrogen bonds.

Hybridizations of A, U, G and C have been compared in different all-valence electron calculations [35], obtaining a hybridization of the carbonyl's oxygen with a nearly $(2p)^2$ orbital in a direction perpendicular to the CO bond. This result, verified here, is insensitive to association (Fig. 10). We find values less far from the classical representation both for NH or NH_2-type ($s^{1.2}p^{2.3}$) and for pyridine-type nitrogens ($s^{1.3}p^{2.8}$).

Table V presents the calculated dipole moments. It has been shown [36] that both semiempirical and *ab initio* methods lead to reasonable consistent predictions for dipole moments of the DNA bases. Let us examine the results for the pairs and triples. Although we cannot ensure quantitative conclusions, the qualitative comparison certainly makes sense.

All the pairs and the triple involving G have higher dipole moments than the other complexes, suggesting thus a possible source of difference in aggregation state, solubility or other properties related to μ. The strikingly high μ values of the G_{15}–C_{48} pair and of the G–G–C triple may play a role in elucidating the tertiary structure through the enhancement of the dipole-monopole and dipole-multipole interactions. These interactions have been extensively analyzed [36, 37].

The direct and reversed A–U pairs lead to similar μ values; so do both pairing schemes for G–U, the wobble and G–U*. The A–A–U triple is not at all equivalent, from the μ viewpoint, to the one including G.

The contribution of $\mu_{orbital}$ is much lower than that of $\mu_{charges}$, as it should be. Nevertheless, in Watson-Crick A–U and C–C they show similar values. It has been claimed [29] that retention of atomic moment is advantageous, for charge moments are usually in poor agreement with experiment and atomic moments generally correct

Table V. Dipole moments μ in Debyes.

	Fig.	$\mu_{tot.}$	$\mu_{charges}$	$\mu_{orb.}$	$\mu_{exp.}$
A (A*)		3.40 (5.86)	2.50 (4.59)	1.39 (1.34)	3.0[a]
U (U*)		5.04 (11.47)	4.01 (7.41)	1.16 (4.24)	4.16[b]
T		5.05	4.33	1.07	4.13[b]
G		8.85	6.02	2.84	
C		9.06	6.63	2.56	7.0[c]
A–T		1.73	2.81	1.34	
A–U	(3a)	1.13	1.81	1.18	
G–C	(3b)	9.42	6.69	2.96	
A–U	(4a)	7.48	5.64	2.18	
A_{14}–U_8	(4b)	6.30	5.25	1.06	
G_{15}–C_{48}	(5a)	18.84	14.51	4.34	
A–C	(5b)	6.11	4.22	1.91	
G_4–U_{69}	(6a)	10.77	7.40	3.54	
G–U*	(6b)	9.78	6.98	3.31	
G_{46}–G_{22}	(7a)	14.83	11.22	3.77	
A–A	(7b)	6.03	5.04	1.06	
C_1–C_2	(8a)	4.96	2.55	2.41	
A*–U*	(8b)	3.46	2.88	0.98	
A_9–A_{23}–U_{12}	(9a)	4.43	3.38	1.31	
G_{46}–G_{22}–U_{12}	(9b)	18.54	13.75	4.82	

[a] H. De Voe and I. Tinoco Jr., J. Mol. Biol. **4,** 500 (1962).
[b] I. Kulakowska, M. Geller, B. Lesing and K. L. Wierzchowski, Biochim. Biophys. Acta **361,** 119 (1975).
[c] I. Kulakowska, M. Geller, B. Lesing, K. Bolewska and K. L. Wierzchowski, Biochim. Biophys. Acta **407,** 420 (1975).

them in the proper direction. It could be argued that in our approximation, as point charges give fairly good agreement with experiment, the correction would be unnecessary. However, taking account of the uncertainties in the few experimental data available, we have chosen to report both values. If it is true that the correction is in the proper direction, then it always increases the charge moment (except for Watson-Crick A–U and A–T, where it decreases); furthermore, it is approximately additive, for the orientation of both vectors turns out to be similar in most cases.

Conclusions

The electron density along a NH ... N bond shows two distinct constant values depending on whether it appears in a Watson-Crick pair or in a Hoogsteen pair: 0.08 of an electron in H ... N in the first one and 0.11 in the second one. In a NH ...O bond, it suffers a large variation, from 0.03 upto 0.08 of an electron in H ... O, independent of the kind of pairing.

I_{NO} exhibits unusually high values for two of the $tRNA^{Phe}$ pairs, the Crick wobble and $G_{15}-C_{48}$. In the wobble, the I_{NO} values are strongly dependent on the pairing positions. For $G_{15}-C_{48}$, the magnified I_{NO} evidences itself through one of the few conjugation curves shown in the experimental electron density maps.

Under triple formation, the I_{XY} corresponding to the hydrogen bonds of the pairs do not weaken, thus contributing to the rigidity of the core region.

Both for pairs and triples, if an oxygen is present the HOMO is almost a pure $2p_\sigma$ oxygen orbital, with coefficient higher than 0.8. LUMO is always π. There is tendency for HOMO and LUMO of pairs to originate from different bases.

All the associations involving guanine have dipole moments significantly higher than the other complexes.

Acknowledgements

We thank Prof. Antonio Julio Lossio Botelho for assisting us with the computations.

[1] F. L. Suddath, G. J. Quigley, A. McPherson, D. Sneden, J. J. Kim, S. H. Kim, and A. Rich, Nature **248,** 20 (1974).
[2] J. D. Robertus, J. E. Ladner, J. T. Finch, D. Rhodes, R. S. Brown, B. F. C. Clark, and A. Klug, Nature **250,** 546 (1974).
[3] D. R. Kearns, Ann. Rev. Biophys. Bioeng. **6,** 477 (1977).
[4] P. D. Johnston and A. G. Redfield, Biochem. **20,** 1147 (1981).
[5] D. Perahia, B. Pullman, D. Vasilescu, R. Cornillon, and H. Broch, Biochim. Biophys. Acta **478,** 244 (1977).
[6] K. Kim and M. S. John, Biochim. Biophys. Acta **565,** 131 (1979).
[7] K. Hoogsteen, Acta Cryst. **12,** 822 (1959).
[8] B. Pullman, P. Claverie, and J. Caillet, Proc. Nat. Acad. Sci. USA **55,** 904 (1966).
[9] B. Pullman, Int. J. Quantum Chem., Quantum Biol. Symp. **4,** 3 (1977).
[10] M. Giambiagi, M. S. de Giambiagi, D. R. Grempel, and C. D. Heyman, J. Chim. Phys. **72,** 15 (1975).
[11] M. Giambiagi, M. S. de Giambiagi, and W. Barroso Filho, Chem. Phys. Lett. **78,** 541 (1981); program from P. Dibout, QCPE **10,** 256 (1973) to which we added the subroutine for bond indices.
[12] M. S. de Giambiagi, M. Giambiagi, and D. M. S. Esquivel, Z. Naturforsch. **37a,** 292 (1982).
[13] A. K. Mukhopadhyay and N. G. Muderjee, Int. J. Quantum Chem. **19,** 515 (1981); S. Beran, Z. Slanina, and D. C. Zidarov, Int. J. Quantum Chem. **19,** 585 (1981).
[14] E. Clementi, J. Mehl, and W. von Niessen, J. Chem. Phys. **54,** 508 (1971).
[15] S. Scheiner and C. W. Kern, J. Am. Chem. Soc. **101,** 4081 (1979).
[16] J. N. Spencer, J. E. Gleim, C. H. Blevins, R. C. Garrett, F. J. Mayer, J. E. Merkle, S. L. Smith, and M. L. Hackman, J. Phys. Chem. **83,** 2615 (1979).
[17] V. Sánchez, A. G. Redfield, P. D. Johnston, and J. Tropp, Proc. Nat. Acad. Sci. USA **77,** 5659 (1980).
[18] C. A. Trindle, J. Am. Chem. Soc. **91,** 219 (1969).
[19] L. Paoloni, J. Chem. Phys. **30,** 1045 (1959).
[20] L. Paoloni, A. Patti, and F. Mangano, J. Mol. Struct. **27,** 123 (1975).
[21] M. Sundaralingam, Int. J. Quantum Chem., Quantum Biol. Symp. **4,** 11 (1977).
[22] B. R. Reid and R. E. Hurd, Acc. Chem. Res. **10,** 396 (1977).
[23] F. H. C. Crick, J. Mol. Biol. **19,** 548 (1966).
[24] G. J. Quigley and A. Rich, Science **194,** 796 (1976).
[25] S. Abdulnur, J. Theor. Biol. **58,** 165 (1976).
[26] G. A. Jeffrey and Y. Kinoshita, Acta Cryst. **16,** 20 (1963).
[27] I. K. Yanson, A. B. Teplitsky, and L. F. Sukhodub, Biopolymers **18,** 1149 (1979).
[28] P. E. Nielsen, Biochim. Biophys. Acta **655,** 89 (1981).
[29] D. B. Boyd, J. Am. Chem. Soc. **94,** 64 (1972).
[30] A. Pullman, M. Dreyfus, and B. Mély, Theor. Chim. Acta Berlin **16,** 85 (1970).
[31] K. Fukui, N. Koga, and H. Fujimoto, J. Am. Chem. Soc. **103,** 196 (1981).
[32] R. Rein and J. Ladik, J. Chem. Phys. **40,** 2466 (1969).
[33] B. Mély and B. Pullman, Theor. Chim. Acta Berlin **13,** 278 (1969).
[34] V. I. Danilov, V. I. Pechenaya, and N. V. Zheltovsky, Int. J. Quantum Chem. **17,** 307 (1980).
[35] A. Pullman, Int. J. Quantum Chem. **IIs,** 187 (1968).
[36] M. N. Stamatadiou, T. J. Swissler, J. R. Rabinowitz, and R. Rein, Biopolymers **11,** 1217 (1972).
[37] B. Pullman and J. Caillet, Theor. Chim. Acta Berlin **8,** 223 (1967).